Influence of AlN passivation on thermal performance of AlGaN/GaN High-Electron Mobility Transistors on Sapphire substrate: A simulation study

P. Murugapandiyan[1], D. Nirmal[2*], Md. Tanvir Hasan[3], Arathy Varghese[4], J. Ajayan[5], A.S. Augustine Fletcher[2], N. Ramkumar[1]

[1] Department of Electronics and Communication Engineering, Anil Neerukonda Institute of Technology & Sciences, Visakhapatnam-India.
[2]Department of Electronics and Communication Engineering, Karunya Institute of Technology and Sciences, Coimbatore, Tamilnadu, India.
[3]Department of Electrical and Electronic Engineering, Jashore University of Science and Technology, Jashore - 7408, Bangladesh.
[4]School of Engineering, Cardiff University, Wales, United Kingdom.

[5]Department of Electronics and Communication Engineering, SR University, Warangal, Telangana, India.

*Corresponding author email:dnirmalphd@gmail.com

Abstract:

This work describes the self-heating effects on the behaviour of AlGaN/GaN-based high-electron Mobility Transistors (HEMTs), which are grown on Sapphire substrate, using electro-thermal TCAD simulations. The proposed device, passivated with AlN/SiN, demonstrates more excellent thermal performance than the conventional one with SiN passivation due to the introduction of additional AlN on top of the device, which acts as a heat spreader. The electro-thermal simulations have carried out for different AlN thicknesses (0 µm to 25 µm), and the device with 5 µm AlN shows better performance compared to others. The proposed AlN/SiN stacked passivation HEMT shows a comparatively small lattice temperature of 418 K, whereas the conventional HEMT with SiN passivation shows 578 K. All the devices (gate length, L_G = 1 µm) switch from OFF- to ON-states using the voltage, V_{GS} from -10 V to 0 V with fixed bias, V_{DS} = 5 V. The values of saturation drain current density (I_{DSS}) and transconductance (g_m) are 0.7 A/mm and 173 mS/mm for the proposed HEMT with 5 µm AlN considering the thermal simulation model. In contrast, the conventional device demonstrates those of 0.42 A/mm and 109 mS/mm, respectively. The ~ 0.32 A/mm of drain current recover for the proposed device with 5 µm AlN from a conventional device because of the reduction of self-heating effects. Our study reveals that the AlN/SiN passivation HEMTs are a promising technology for high-power switching and microwave applications without significant reduction in device performance at high drain bias.

Keywords:

Self-heating; lattice temperature; AlN; thermal management; sapphire; DC characteristics; HEMT;

1. Introduction:

Nowadays, GaN-based HEMTs have attracted enormous attention for high-power and high-frequency applications [1-4]. Due to their high breakdown field and wider bandgap, GaN-based heterostructure devices have been proved to have high-power handling capability to withstand excessive temperatures and corrosive ambient [5]. These devices have gained colossal research focus because of their exemplary performance in terms of very high saturation velocities of the charge carriers and enormous charge densities achieved even without intentional doping, the breakdown voltage of few 100's of volts, and operational frequencies ranging from few GHz to THz [6-9]. The GaN HEMTs have already achieved a commercial breakthrough in optical, RF device, and power markets. However, the self-heating effects (SHEs), increase in crystal temperature, by the elevated lattice temperature at high-power operation limits the device performance by the degradation of electron mobility, breakdown voltage, and radio frequency (RF) characteristics [10-14]. The SHEs have hindered the manufacturing of high-quality HEMTs that become dominant when drain bias is applied, leading to sub-optimal breakdowns. Extensive researches have been conducted to overcome the SHEs by various research groups using advanced field plate structures, excessive thermal stability material, and air-water cooling device framework [15-19]. However, even after lots of research, an optimized device has not been proposed to meet the market power-requirements. Almost all of the HEMT designs are found to have the limitation of a suboptimal breakdown even when the GaN material has a very high breakdown field of 3 MV/cm [20-22]. Usually, GaN has grown on the substrate, such as Sapphire, Si, and SiC, for high-power applications. Though the SiC has high thermal conductivity (TC) (330 W/m-K @ room temperature, RT), the costs and lack of availability in large sizes and ~13% mismatch in the lattice parameter for GaN on SiC [23] are the bottlenecks of SiC substrate. On the other hand, Si material is available in larger wafer size at low costs, and its more excellent TC (150 W/m-K at RT) makes it one of the choices. However, due to the non-mature process technologies for GaN-on-Si combined with a high-lattice mismatch (~16%) and significant difference in thermal expansion coefficients (where the values of 2.6×10^{-6} K^{-1} and 5.59×10^{-6} K^{-1} for Si and GaN, respectively), Si substrate reduces the reliability of the devices. Besides, the AlN nucleation layer or multiple layers of AlN and AlGaN with varying concentrations of Al forming a transition scheme are necessary to reduce the lattice mismatch for GaN grown on Si [24,25]. Despite low-TC (42 W/m-K at RT), many research-groups have recently demonstrated the outstanding performance of the GaN-material based devices with the sapphire substrate [23-32]. Therefore, sapphire has become an excellent choice as a substrate due to its high crystalline quality, lattice constant matching with GaN, low cost of wafers, and availability in larger wafer sizes.

Theoretical and experimental results have strongly confirmed that reduction of SHEs on AlGaN/GaN-based devices are a critical issue in various regards. Varghese et al. demonstrated that the AlGaN/GaN HEMTs exhibited outstanding device performance due to the introduction of triple AlN inter-layers, those employed as a spacer layer, nucleation layer, and interfacial passivation [25]. Huang et al. claimed that the decrease of dynamic ON-resistance and current-collapse suppression seen in AlGaN/GaN HEMTs with the AlN passivation [33]. Several research groups reported various techniques for thermal optimization for GaN-based devices and circuits. Dasom Jeon et al. demonstrated the reduction of self-heating in nano-interfaces by using h-BN based 2D interface [34]. GaN on Si substrate HEMTs based RF amplifier thermal dissipation improved by plastic package [35]. Etched AlGaN barrier HEMTs reduces the channel temperature by generating a new hot-spot in the thermal field [36]. Neama et.al. demonstrated a thermal management technique for GaN-HEMTs using mini-channel heat sinks [37]. A copper filled Micro-Trench structure used for thermal management of GaN on Si HEMT [38]. Different passivation materials had been employed to reduce the SHEs of GaN HEMTs [39-41]. Chander et al. studied the SHEs of AlGaN/GaN HEMT with field plate structure on SiC substrate for different passivation materials [39]. Haghshenas et al. reported that the passivation thickness and material had a significant role in the hot spot temperature of AlGaN/GaN HEMTs with a single passivation layer [40]. Our previous works reported the effective suppressing of SHEs on AlGaN/GaN-based HEMT with the filed-plated structure on SiC substrate using stacked passivation [41]. Still, inadequate data on the SHEs on the device performance are available, and studies on AlGaN/GaN HEMTs grown on sapphire substrate with stacked passivation are lacking. However, such results are vital to design the next-generation high-power and high-frequency devices. Therefore, a more detailed understanding and the proper inclusions of the SHEs on device performance are immensely crucial.

In this work, we proposed a cost effective AlN/SiN stacked passivation for thermal optimization of GaN-HEMTs grown on sapphire substrate. We have explored the electro-thermal analysis of AlGaN/GaN HEMTs using TCAD simulations on the SILVACO ALTAS platform [42] for with and without top AlN layer. TCAD simulations carry out with and without a self-heating model. Both lateral- and vertical-lattice temperatures of devices are also studied. The proposed device shows promising results compared to a conventional one due to better heat dissipation, which is achieved by introducing AlN on top. The AlN layer in the passivation scheme reduces interface traps at passivation/AlGaN and plays a vital role in enhancing the drain current by lowering the SHEs. All the simulations have been done at room temperature.

2. Materials, Methods, and Models

The illustrations of GaN/AlGaN HEMTs without (conventional) and (proposed) top AlN are demonstrated in Fig. 1(a) and (b), respectively. Fig. 1 (c) demonstrates the expected device fabrication process steps. The composition, x = 0.25 is consider for the barrier layer, $Al_xGa_{1-x}N$. The geometric and material parameters are provided in Table I and Table II, respectively. The conventional device defines as an GaN/AlGaN HEMT with SiN passivation, whereas the GaN/AlGaN HEMT with dual passivation, AlN/SiN, is the proposed device. The conventional device has been simulated without and with the self-heating model, which define as CM (conventional model simulation) and SHM (self-heating model simulation), respectively. The simulations have been done with the proposed self-heating model, which is mentioned as SHM with AlN.

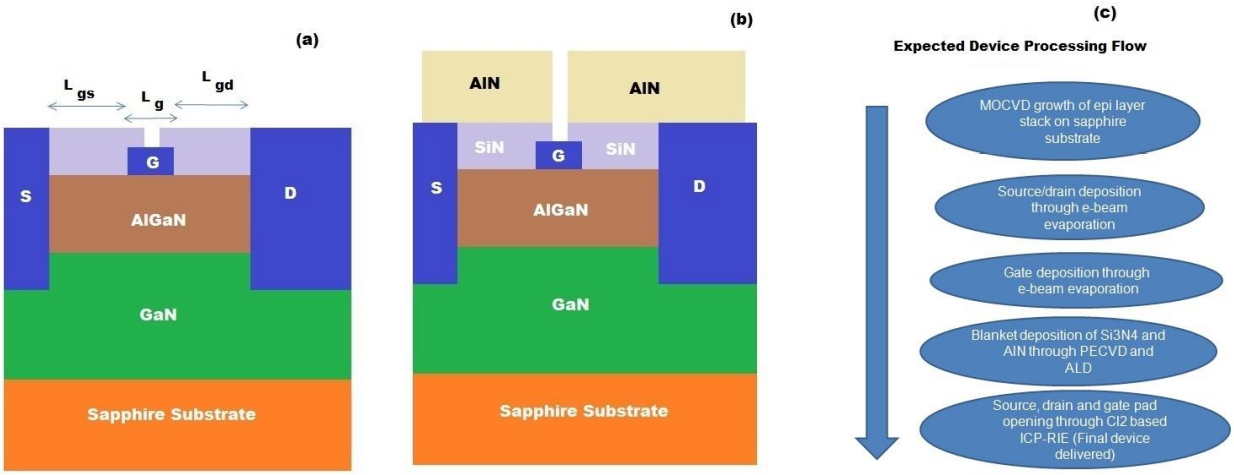

Figure 1(a). Illustrations of a conventional GaN/AlGaN-HEMT. Figure 1(b). Illustrations of the proposed device design with AlN layer on top. Figure 1(c). Process flow to make feasible the proposed device fabrication.

Table I. Geometric parameters

Parameter	Value
AlGaN barrier layer thickness	**26.7 nm**
GaN channel layer thickness	**47.3 nm**
GaN buffer layer thickness	**1.0 µm**
SiN passivation thickness	**5.5 µm**
Top AlN	**0 ~ 25 µm**
L_G (length of gate)	**1.0 µm**
L_{sg} (distance between source & gate)	**2.0 µm**
L_{gd} (distance between gate & drain)	**2.0 µm**
Gate Width (W)	**100 µm**

A two-dimensional (2D) TCAD simulation is carried out using lattice temperature model to investigate the self-heating-effects (SHEs) of GaN/AlGaN HEMT. Additionally, we consider the essential physical models such as interface trap models, surface trap state model, nitride low & high field mobility models, and SRH (Shockley–Read–Hall) recombination models. The thermal boundary resistances (TBRs) are considered for each material in the simulation [42-50].

Table II. Material parameters

Parameter	GaN	AlGaN
E_g (Semiconductor band gap in eV)	3.4	3.96
µ (Low field electron mobility in $cm^2/V.s$)	1460	300
ε_r (Relative permittivity)	9.5	9.5
Saturation velocity of electron in cm/S	2×10^7	1.12×10^7
Electron affinity (eV)	4	3.82
Saturation velocity of hole in cm/S	1.9×10^7	1.0×10^6

Conduction band DOS ($\times 10^{18}$) in cm^{-3}	1.07	2.07
SRH lifetime	1.0×10^{7}	1.0×10^{7}
Valence band DOS ($\times 10^{19}$) in cm^{-3}	1.16	1.16

DOS: Density of states; SRH: Shockley Read Hall Recombination

DD (Drift-Diffusion) model of charge transport, Fermi-Dirac, Boltzman carrier statistics & interface traps models are used in this work, which is adequate for all micrometer range devices that are technologically feasible. The more conventional form of drift-diffusion equations are as follows [42]:

$$J_n = qn\mu_n E_n + qD_n\nabla_n \quad (1)$$

$$J_p = qp\mu_p E_p - qD_p\nabla_p \quad (2)$$

Where μ_n and μ_p are electron and hole mobility, respectively, and E stands for the effective electric field.D_n and D_p are written as [42]:

$$D_n = \frac{kT_L}{q}\mu_n \quad (3)$$

$$D_p = \frac{kT_L}{q}\mu_p \quad (4)$$

Where T_L & k represents lattice temperature & Boltzman constant respectively. The self-heating model includes the primary lattice heat flow model, heat generation and recombination models, and thermal conductivity model [42]:

Lattice heat flow [42]:

$$C_{th}\frac{\partial T_L}{\partial t} = \nabla(k\nabla T_L) + H \quad (5)$$

Where C_{th} & k respectively represents the thermal capacitance & TC (thermal conductivity). In general, the electro-thermal effects are modeled by thermal capacitance $C_{th} = \frac{\Delta Q\ (rate\ of\ change\ of\ heat\ flow)}{\Delta T\ (rate\ of\ change\ of\ temperature)}$ and thermal resistance R_{th} parallel network consists of thermal current source (I_{diss}). High thermal conductivity of the semiconductors transports the generated heat energy faster than lower TC materials and R_{th} is the TC dependent parameter.

Heat generation and recombination [42]:

$$H = \left(\frac{\left|\overrightarrow{Jn}\right|^2}{q\mu_n n} + \frac{\left|\overrightarrow{Jp}\right|^2}{q\mu_p p}\right) + q(R-G)[\varphi_p - \varphi_n + T_L(P_p - P_n)] \quad (6)$$

Thermal conductivity [42]:

$$k(T_L) = (TC.CONST)/(T_L/300)^{TC.NPOW} \quad (7)$$

The Material thermal conductivity constant is $TC.NPOW$ and the thermal resistance$\left(R_{th} = \frac{\Delta T(riseinthechanneltemperature)}{P_{diss}}\right)$ links the channel temperature to power dissipation. The thermal constants are listed in Table III.

Temperature dependent nitride low field mobility model [39]:

$$\mu_0(T,N) = \mu_{min}\left(\frac{T}{300}\right)^{\beta_1} + \frac{(\mu_{max}-\mu_{min})\left(\frac{T}{300}\right)^{\beta_2}}{1+\left[\frac{N}{N_{ref}\left(\frac{T}{300}\right)^{\beta_3}}\right]^{\alpha(T/300)^{\beta_4}}} \quad (8)$$

Where N & T indicates the total doping density & temperature respectively and α, β_1, β_2, β_3, β_4,μ_{min}, μ_{max}, and N_{ref} are fitting parameters [42].

Table III. Thermal conductivity constant [42]

Parameter	Unit	AlGaN	GaN	AlN	Sapphire
Thermal conductivity constant ($TC.CONST$)	W/cm-k	0.4	1.3	1.8	0.3

Nitride high field mobility (temperature dependent) model [42]:

$$\mu = \frac{\mu_0(T,N)+v^{sat}\frac{E^{n1-1}}{E_c^{n1}}}{1+a\left(\frac{E}{E_c}\right)^{n2}+\left(\frac{E}{E_c}\right)^{n1}} \qquad (9)$$

Where, μ_0 & E indicates the low field mobility & electric field respectively, v^{sat}, E_c, $n1$, $n2$ and a are fitting parameters of Faramand modifier Thomas Nitride model [42].

SRH (Shockley-Read Hall) Model [42]:

$$R_{SRH} = \frac{pn-n_{ie}^2}{TAUP0\left[n+n_{ie}\exp\left(\frac{ETRAP}{kT_L}\right)\right]+TAUN0\left[p+n_{ie}\exp\left(\frac{ETRAP}{kT_L}\right)\right]} \qquad (10)$$

Where,$ETRAP$ is the difference in energy levels between trap state and Fermi level, and the electron & hole lifetimes are denoted by $TAUN0$ and $TAUP0$ respectively. The electron & hole carrier concentrations (cm^{-3}) are defined as n and p, respectively. The n_{ie} is an effective intrinsic concentration. T_L and k are defined as lattice temperature and Boltzmann constant, respectively [42].

3. Results and discussions

The DC output characteristics of conventional HEMT has been done without incorporating the thermal models for gate bias (V_{GS}), swept from 0 V to -5 V and drain-bias (V_{DS}), swept from 0 V to 15 V (Fig.2 (a)). The peak I_{DS} is ~1.2 A/mm at the bias voltage of V_{GS} = 0 V and V_{DS} = 15 V. The extracted 2-DEG (2-dimensional electron gas) and mobility (μ) of the channel are 1.14×10^{13} cm^{-2} and 1260 cm^2/V-s, respectively. Figures 2 (b) and (c) demonstrate the device characteristics of conventional and proposed HEMTs with self-heating model, respectively. The value of drain current dispersion is higher for the conventional devices as compared with the proposed one. This result can be reasoned by the SHE (self-heating effect) that becomes dominant in the conventional device at higher drain biases, leading to noticeable degradation in the current density. The conventional device shows a peak current of 0.42 A/mm at V_{GS} = 0 V. As a result of self-heating effects, an increase in lattice temperature by an applied electric field and thus thermal scattering and degradation in the electron mobility occurs. At high drain voltage, the effect of scattering of the carriers increased, and therefore in the region of saturation, there will be a negative slope of drain current. Figure 2 (c) represents the proposed device's output characteristics with SHM for 5 μm AlN thickness. Inclusion of AlN with high TC of 1.8 W/cm-K as a heat spreader in the conventional HEMT reduces the SHEs in the device channel's access

region, thereby improving the normalized drain current density to 0.7 A/mm at V_{GS} = 0 V. Besides, this also reduces the electron traps in the device.

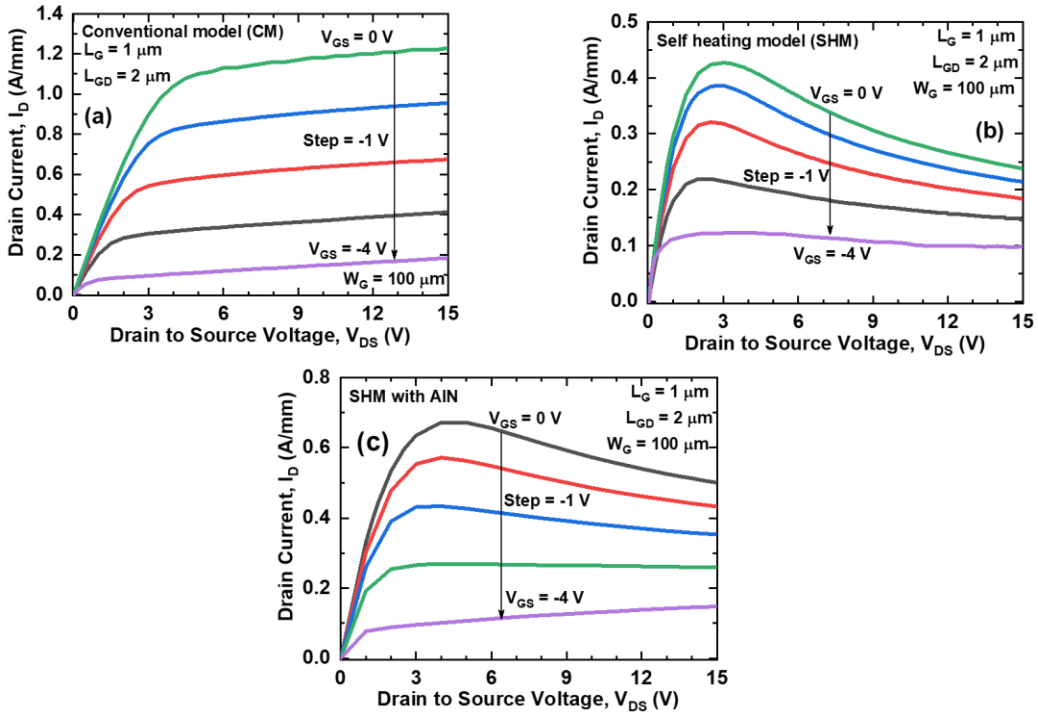

Figure 2. DC characteristics of conventional and proposed HEMTs with L_G = 1 µm. The characteristics are shown as (a) conventional device without self-heating model (SHM), (b) conventional device with self-heating model (SHM), and (c) proposed device with self-heating model (SHM) for 5 µm AlN thickness.

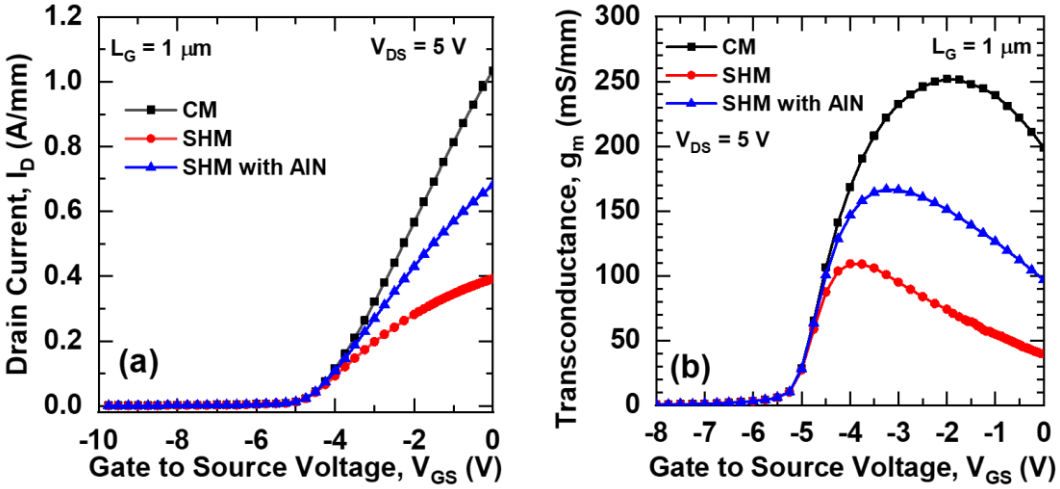

Figure 3. Transfer (a) and transconductance (b) characteristics of a conventional device without self-heating model (SHM), a conventional device with self-heating model (SHM,) and the proposed device with self-heating model (SHM) for 5 µm AlN thickness.

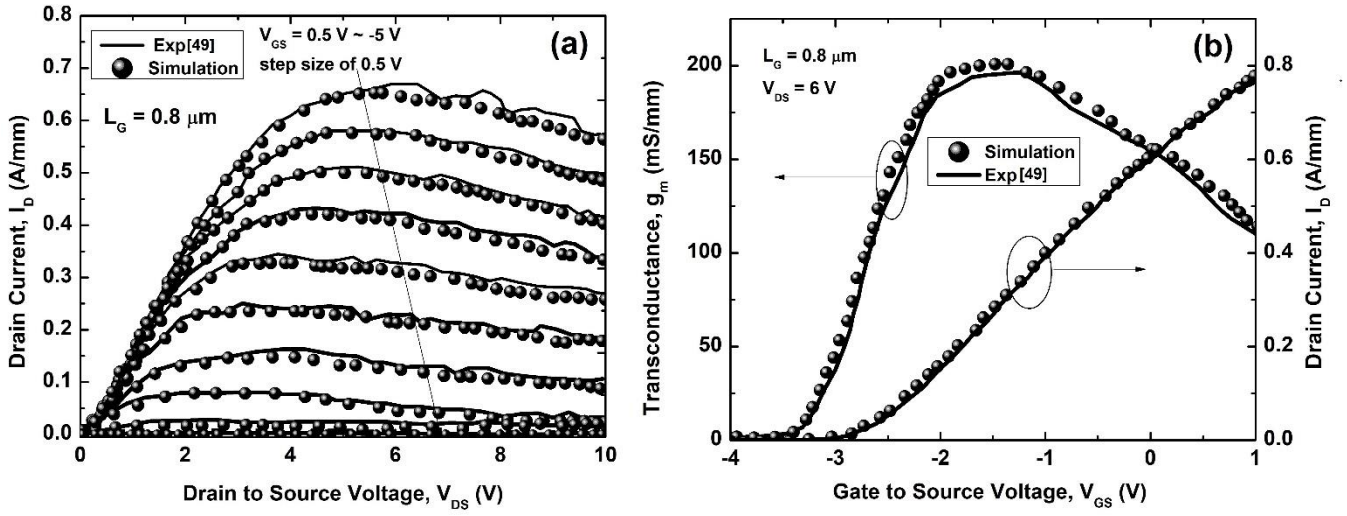

Figure 4(a). DC characteristics of conventional AlGaN/GaN HEMT on sapphire substrate with a L_G = 0.8 µm [49]. Figure 4(b). Transfer characteristics.

Fig.3 (a) demonstrates the comparison of transfer curves of a conventional HEMT, a conventional HEMT with self-heating model simulation (SHM), and the proposed device with self-heating model (SHM) for V_{GS} swept from -10 V to 0 V and V_{DS} = 5 V. Fig.3 (b) shows the transconductance characteristics of the conventional device, the conventional device with self-heating model simulation, and proposed device with self-heating model simulation for 5 µm AlN thickness for V_{GS} swept from -10 V to 0 V at fixed drain bias, V_{DS} = 5 V. It is found that there is a significant drop in the both I_{DS} and g_m for the devices with self-heating model simulation. The off-state gate leakage currents are 3.3×10^{-16} A/mm, 1.4×10^{-9} A/mm, and 2.1×10^{-12} A/mm for a conventional device without self-heating model simulation, a conventional device with self-heating model simulation, and the proposed device with self-heating model simulation, respectively. The peak values of transconductance (g_m) are 273 and 109 mS/mm for a conventional device with and without self-heating model simulation. In comparison, it shows 173 mS/mm for the proposed device with the top 5 µm AlN for self-heating model simulation. The threshold voltages are almost the same as – 5 V for all the devices.

The increase of crystal temperature causes thermal scattering, which diminished the electrons' mobility in the channel. Further, at high drain voltage, the SHE increased, reducing the I_{DS} and g_m. The overall output current density and the maximum transconductance improved in the proposed device with AlN passivation thermal structures. TCAD simulation is carried out for L_G = 0.8 µm GaN/AlGaN HEMT on the sapphire substrate reported in [49], and it is DC, and transfer curves are displayed in Fig.4 (a) and Fig 4(b), respectively. The results show a perfect match with experimental results.

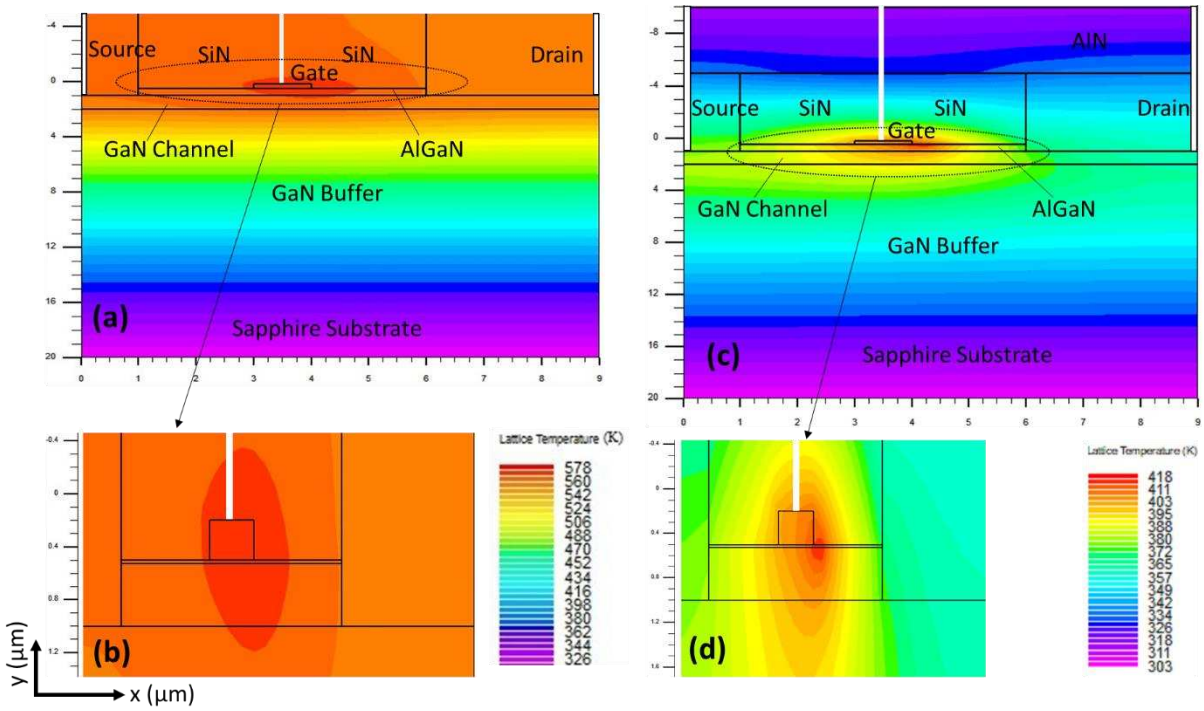

Figure 5(a). Temperature gradient profile of conventional device with self-heating model simulationfor drain bias (V_{DS}) 15 V. Figure 5(b). Channel temperature gradient profile of conventional device with self-heating model simulation. Figure 5(c). Temperature gradient profile of proposed device with self-heating model simulation for 5 μm AlN top layer. Figure 5(d). Channel temperature gradient profile of proposed devices with self-heating model simulation for 5 μm AlN top layer.

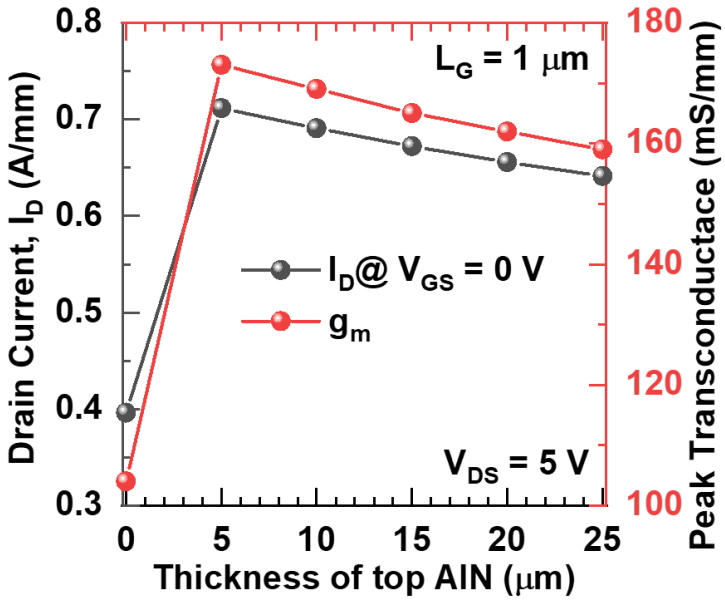

Figure 6. Effect of top AlN thickness on drain current and peak transconductance

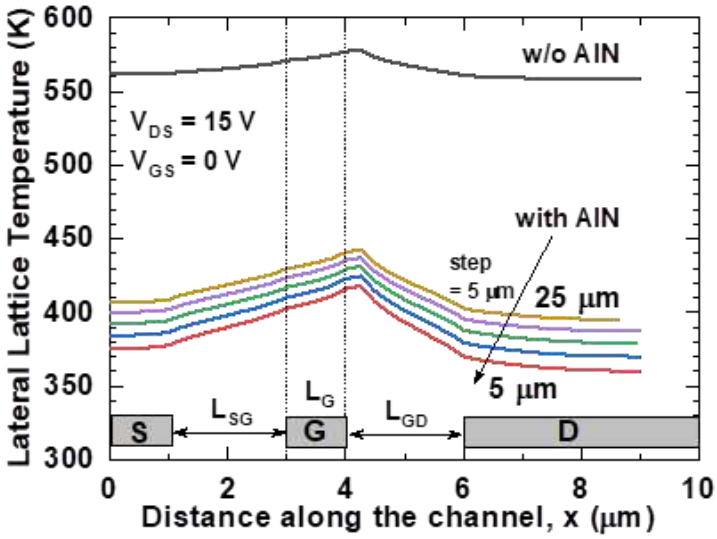

Figure 7. Lattice temperature variation along the channel, *x* of the conventional device, and the proposed device with self-heating model simulation for different AlN thickness.

The temperature gradient profile of a conventional device with self-heating model simulation at V_{GS} = 0 V and V_{DS} = 15 V is depicted in Fig. 5 (a). A maximum lattice temperature of 578 K is observed in the device (Fig.5 (b)). The proposed device's temperature gradient profile with SHM for 5 µm AlN is demonstrated in Fig.5(c). The peak-temperature of 418 K observed in the device, as shown in Fig. 5(d). TCAD simulation of the device's temperature gradient profile with 20 µm Sapphire substrate and 5 µm AlN thicknesses is presented in Fig.5. However, TCAD simulation is performed for various substrate thicknesses (20 µm to 300 µm) and confirmed that the device characteristics and channel temperature profile are the same for various substrate thicknesses for a particular AlN top layer thickness. The top AlN thickness-dependent drain current and transconductance are depicted in Fig. 6. The I_{DS} is enhanced due to the introduction of AlN on top. However, it starts to reduce above 5 µm by increasing AlN's thickness, and similar effects are observed in transconductance. The proposed device shown high drain current and transconductance for 5 µm AlN thickness results from reduced lattice temperature shown in Fig. 7.

Comparative lattice temperature variation along the channel of a conventional device with self-heating model simulation and proposed device with self-heating model simulation for different thicknesses of top AlN is shown in Fig 7. The overall vertical lattice temperature distribution of region near the gate end of the drain side of conventional and proposed devices is shown in Fig. 8(a) and Fig. 8(b), respectively. Figure 8 (c) shows the effects of the top AlN thickness on vertical lattice temperature. The

proposed device near the gate electrode showed the low lattice temperature. The additional AlN passivation effectively decreases the temperature in 2DEG. As a result, the proposed thermal structure improved the overall DC characteristics.

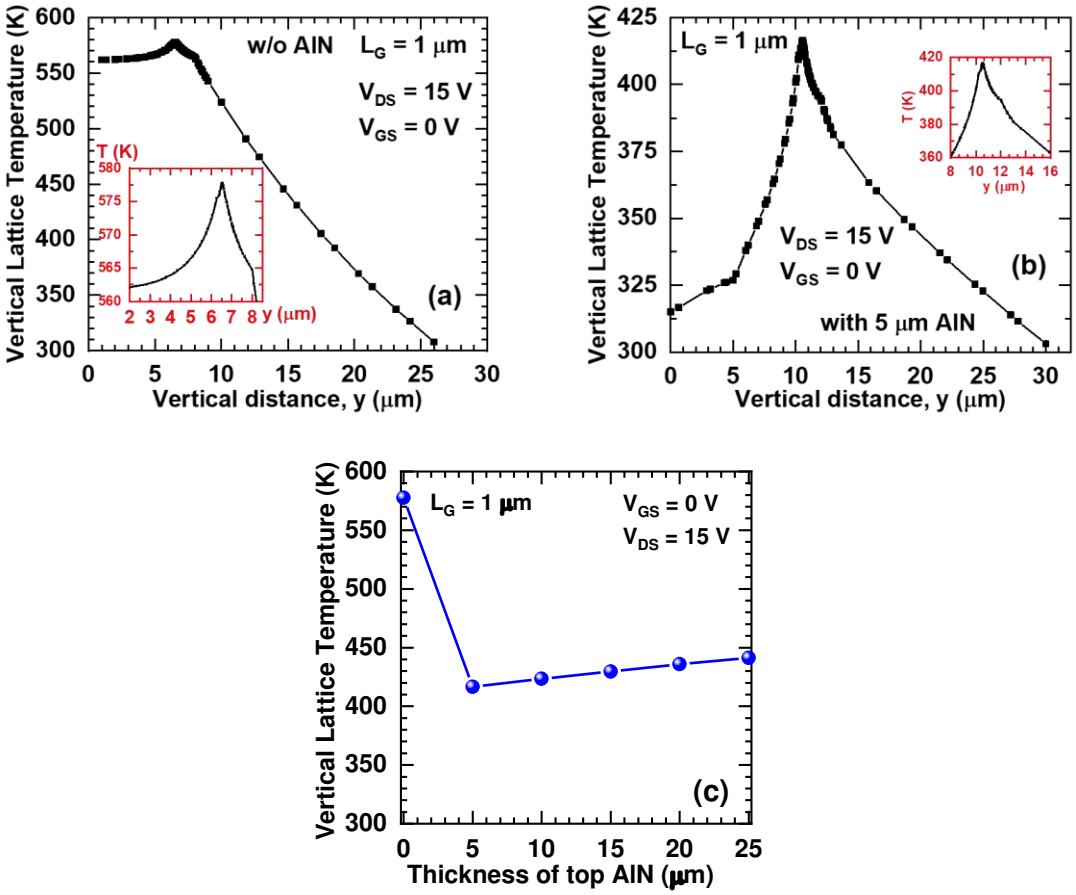

Figure 8. Vertical lattice temperature gradient of the conventional (a) and the proposed (b) devices with self-heating model simulation. Inset figures show the enlarged view of the region near the gate end of drain side. Figure 8 (c) effects of the top AlN thickness on vertical lattice temperature.

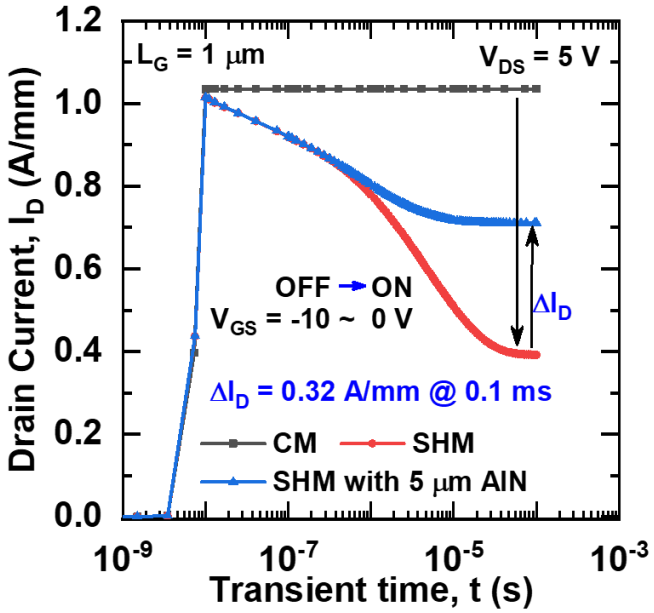

Figure 9. Transient time drain current responses of a conventional device with and withoutself-heating model simulation, and the proposed device with self-heating model simulation for 5 µm AlN top layer.

Fig. 9 shows the transient characteristics of the current drain, I_D for AlGaN/GaN HEMTs with different models. The devices switch from OFF-state (V_{GS} = -10 V) to ON-state (V_{GS} = 0 V) with a fixed V_{DS} = 5 V. The devices show different times when the I_{DS} reached a steady state at the same electric bias. The conventional AlGaN/GaN HEMT transient current drops significantly using self-heating model simulation due to temperature rise in the channel when it reaches steady-state conditions. Wang et al. [49], Zhang et al. [50] and Yachao Zhang et al. [51] reported that the current drop in the GaN/AlGaN HEMTs occurred for the reduction of electron mobility in the channel. One of the key factors of this reduction is self-heating in the devices. At the very beginning of switching, the devices show almost the same drain current using the thermal models and start to change with the time due to reduction of the channel mobility, caused by self-heating. However, the thermal optimized HEMT using a high thermal conductivity AlN passivation (5 µm) has shown improved I_D transient response of Δ_{ID} = 0.32 A/mm at 0.1 ms. The above results indicate that the additional AlN deposited on SiN passivation improves the performance device due to the reduction of SHEs.

4. **Conclusion**

The studies of self-heating effects on AlGaN/GaN HEMT DC characteristics with a dual SiN/AlN passivation have been presented. The proposed thermally optimized HEMT device design incorporating an AlN passivation layer significantly improved the device's electrical characteristics over the conventional ones. The overall device temperature in crystal lattice within the 2DEG channel and temperature in the vertical lattice is found to get reduced due to the temperature handling capability of AlN. An investigation of the impact of AlN thickness on device performance has been presented. The drain current, transconductance, and proposed device are also improved compared to the conventional one. The proposed dual SiN/AlN passivation HEMT (L_G = 1µm) TCAD simulation with self-heating model shown 60% improvement in drain current density and 63% improvement in transconductance. The device's overall performance is enhanced with the incorporation of 5 µm AlN making the device reliable and stable for a wider range of operation, which is desirable in the high-power domain.

Data availability

The raw/processed data required to reproduce these findings cannot be shared at this time as the data also forms part of an ongoing study.

References:

[1] P. Murugapandiyan, S. Ravimaran, J. William, J. Ajayan and D. Nirmal (2017) DC and microwave characteristics of 20 nm T-gate InAlN/GaN high electron mobility transistor for high power RF applications. Superlattices and Microstructures 109:725 - 734. doi: 10.1016/j.spmi.2017.05.060.

[2] P. Murugapandiyan, S. Ravimaran, J. William, and K. Meenakshi Sundaram. (2017) Design and Analysis of 30 nm T-Gate InAlN/GaN HEMT with AlGaN back-barrier for High power Microwave Applications. Superlattices and Microstructures 111:1050-1057 doi:10.1016/j.spmi.2017.08.002.

[3] A.S. AugustineFletcher, and D.Nirmal. (2017)A survey of Gallium Nitrate HEMT for RF and high power applications Superlattices and Microstructures 109:519-537doi:http://dx.doi.org/10.1016/j.spmi.2017.05.042

[4] BinolaK.Jebalin, A.ShobhaRekh, P.Prajoon, D.Godwinraj, N.Mohan Kumar, and D.Nirmal. (2015) Unique model of polarization engineered AlGaN/GaN based HEMTs for high power applications. Superlattices and Microstructures 78:210-223do:10.1016/j.spmi.2014.10.038

[5] Kirschman, Randall K,High-Temperature Electronics, NY: IEEE Press,2000, ISBN 0-7803-3477-9.

[6] Shen, L.; Heikman, S.; Moran, B.; Coe, R.; Zhang, N.Q.; Buttari, D.; Smorchkova, I.P.; Keller, S.; DenBaars, .P.; Mishra, U.K (2001) AlGaN/AlN/GaN high-power microwave HEMT. IEEE Electron Device Lett 22:457–459.https://doi.org/10.1109/55.954910

[7] Yang Lu, Xiaohua Ma, Ling Yang, Bin Hou, Minhan Mi, Meng Zhang, Jiaxin Zheng, Hengshuang Zhang, and Yue Hao. (2018) High RF Performance AlGaN/GaN HEMT Fabricated by Recess-Arrayed Ohmic Contact Technology. 39(6): 811-814 https://doi.org/10.1109/LED.2018.2828860

[8] Del Alamo, J.A.; Joh, J. GaN HEMT reliability. Microelectron. Reliab (2009) GaN HEMT reliability49:1200–1206. https://doi.org/10.1016/j.microrel.2009.07.003

[9] Mishra, U.K.; Parikh, P.; Wu, Y.F.(2002) AlGaN/GaN HEMTs-an overview of device operation and applications. Proc. IEEE, 90:1022–1031. https://doi.org/10.1109/JPROC.2002.1021567.

[10] Lu, W.; Yang, J.; Khan, M.A.; Adesida, I. (2001) AlGaN/GaN HEMTs on SiC with over 100 GHz f/sub T/and low microwave noise. IEEE Trans. Electron Devices 48:581–585. https://doi.org/10.1109/16.906454

[11] Gaska, R.; Osinsky, A.; Yang, J.W.; Shur, M.S. (1998) Self-heating in high-power AlGaN-GaN HFETs. IEEE Electron Device Lett., 19:89–91 https://doi.org/10.1109/55.661174.

[12] Wang, X.D.; Hu,W.D.; Chen, X.S.; Lu, W. (2012) The study of self-heating and hot-electron e_ects for AlGaN/GaN double-channel HEMTs. IEEE Trans. Electron Devices 59:1393–1401 https://doi.org/10.1109/TED.2012.2188634.
[13] Sadi, T.; Kelsall, R.W.; Pilgrim, N.J. (2006) Investigation of self-heating effects in submicrometerGaN/AlGaN HEMTs using an electrothermal Monte Carlo method. IEEE Trans. Electron Devices, 53:2892–2900.https://doi.org/10.1109/TED.2006.885099.
[14] Hwang, I.T.; Jang, K.W.; Kim, H.J.; Lee, S.H.; Lim, J.W.; Yang, J.M.; Kwon, H.S.; Kim, H.S (2019) Analysis of DC Characteristics in GaN-Based Metal-Insulator-Semiconductor High Electron Mobility Transistor with Variation of Gate Dielectric Layer Composition by Considering Self-Heating Effect. Appl. Sci., 9, 3610. https://doi.org/10.3390/app9173610.
[15] Kwak, H.T.; Chang, S.B.; Jung, H.G.; Kim, H.S (2018) Thermal analysis of AlGaN/GaN high-electron-mobility transistor and its RF power efficiency optimization with source-bridged field-plate structure. J. Nanosci. Nanotechnol 18:5860–5867.https://doi.org/10.1166/jnn.2018.15572.
[16] Kwak, H.T.; Jang, K.W.; Kim, H.J.; Lee, S.H.; Lim, J.W.; Kim, H.S (2019) DC Characteristics of AlGaN/GaN High-Electron Mobility Transistor with a Bottom Plate Connected to Source-bridged Field Plate Structure. J. Nanosci. Nanotechnol. 19:2319–2322 https://doi.org/10.1166/jnn.2019.16004.
[17] Wang, A.; Tadjer, M.J.; Calle, F. (2013) Simulation of thermal management in AlGaN/GaN HEMTs with integrated diamond heat spreaders. Semicond. Sci. Technol., 28:055010 https://doi.org/10.1088/0268-1242/28/5/055010.
[18] Kim, H.J.; Jang, K.W.; Kim, H.S. (2019) Operational Characteristics of Various AlGaN/GaN High Electron Mobility Transistor Structures Concerning Self-Heating Effect. J. Nanosci. Nanotechnol 19: 6016–6022https://doi.org/10.1166/jnn.2019.17006.
[19] Kwak, H.T.; Chang, S.B.; Kim, H.J.; Jang, K.W.; Yoon, H.; Lee, S.H.; Lim, J.W.; Kim, H.S (2018) Operational Improvement of AlGaN/GaN High Electron Mobility Transistor by an Inner Field-Plate Structure. Appl. Sci. 8:974https://doi.org/10.3390/app8060974.
[20] Yan, Z.; Liu, G.; Khan, J.M.; Balandin, A.A. (2012) Graphene quilts for thermal management of high-power GaN transistors. Nat. Commun. 3:827 https://doi.org/10.1038/ncomms1828.
[21] S. Vitanov, V. Palankovski, S. Maroldt, and R. Quay (2010) High-temperature modeling of AlGaN/GaN HEMTs, Solid-State Electronics, 31: 54(10):1105-12 https://doi.org/10.1016/j.sse.2010.05.026
[22] Naiqian Zhang, (2002) High Voltage GaN HEMTs with Low on-resistance for Switching Applications. PhD thesis, University of California, Santa Barbara
[23] B. Benbakhti, A. Soltani, K. Kalna, M. Rousseau and J. De Jaeger. (2009) Effects of Self-Heating on Performance Degradation in AlGaN/GaN-Based Devices, IEEE TRANSACTIONS ON ELECTRON DEVICES, 56(10):2178- 2185 doi:10.1109/TED.2009.2028400.
[24] Varghese, A., Periasamy, C., Bhargava, L., Dolmanan, S.B. and Tripathy, S.,(2019) Linear and Circular AlGaN/AlN/GaN MOS-HEMT-based pH Sensor on Si Substrate: A Comparative Analysis. IEEE Sensors Letters, 3(4):1-4 https://doi.org/10.1109/LSENS.2019.2909291
[25] Arathy Varghese, ChinnamuthanPeriasamy, Lava Bhargava, and K. Vijayakumar (2018) Impact of AlN Interlayer's in Epitaxial and Passivation Scheme on the DC and Microwave Performance of Doping-Less GaN HEMT, Journal of Nanoelectronics and Optoelectronics, 13(7): 971-979 https://doi.org/10.1166/jno.2018.2308.
[26] JiejieZhu ,Siqi Jing, Xiaohua Ma , Siyu Liu, Pengfei Wang, Yingcong Zhang, Qing Zhu , Minhan Mi , Bin Hou , Ling Yang , Martin Kuball , and Yue Hao (2020) Improvement of Electron Transport Property and ON-Resistance in Normally-OFF Al2O3/AlGaN/GaN MOS-HEMTs Using Post-Etch Surface Treatment , IEEE TRANSACTIONS ON ELECTRON DEVICES 67(9):3541 – 3547 doi:10.1109/TED.2020.3007564
[27] Grigelionis, I.; and Kašalynas, I. (2020) Terahertz Spectroscopy of Thermal Radiation from AlGaN/GaN Heterostructure on Sapphire at Low Temperatures ,Applied Sciences, 10:851 doi:10.3390/app10030851
[28] N. Gao, N. Gao, Y. L. Fang, J. Y. Yin, B. Wang, Y. M. Guo, Z. Z. He, G. D. Gu, H. Y. Guo, Z. H. Feng, and S. J. Cai. (2017) Comparison of AlGaN/GaN HEMTs Grown and Fabricated on Sapphire Substrate with AlN and GaN Nucleation Layers, IEEE Proceedings, 978-1-5386-4851-3 doi: 10.1109/IFWS.2017.8246009
[29] Sheng Jiang,Yuefei Cai, Peng Feng, Shuoheng Shen, Xuanming Zhao, Peter Fletcher, Volkan Esendag, Kean-Boon Lee, and Tao Wang. (2020) Exploring an Approach toward the Intrinsic Limits of GaNElectronics ,Applied Materials & Interfaces,12: 12949 – 12954 doi:10.1021/acsami.9b19697
[30] Takushi Kaneko, Narihito Okada, and Kazuyuki Tadatomo. (2020) Effect of InGaN/GaN Superlattice on Lattice Curvature of GaN Layers Grown on Sapphire Substrates, physica solidi status b, 257:1900586 doi:10.1002/pssb.201900586.
[31] Yachao Zhang, Yifan Li, Jia Wang, Yiming Shen, Lin Du, Yao Li, Zhizhe Wang, Shengrui Xu, Jincheng Zhang and Yue Hao, Zhang. (2020) High performance AlGaN Double Channel HEMTs with Improved Drain current Density and High Breakdown Voltage , *Nanoscale Res Lett* ,15:114doi:10.1186/s11671-020-03345-6
[32] K Takhar, U P Gomes, K Ranjan, S Rathi and D Biswas. (2015) Temperature dependent DC characterization of InAlN/(AlN)/GaN HEMT for improved reliability, Mater. Sci. Eng. 73:012001 doi:10.1088/1757-899X/73/1/012001

[33] S. Huang, Q. Jiang, S. Yang, C. Zhou and K. J. Chen. (2012) Effective Passivation of AlGaN/GaN HEMTs by ALD- Grown AlN Thin Film, IEEE Electron Device letters 33(4): 516 – 518 doi: 10.1109/LED.2012.2185921.

[34] Dasom Jeon, Jinho Lim, Junho Bae, Arman Kadirov, Yongsu Choi, Seunghyun Lee, Suppression of self-heating in nanoscale interfaces using h-BN based anisotropic heat diffuser, Applied Surface Science, Volume 543, 2021, https://doi.org/10.1016/j.apsusc.2020.148801.

[35] R. Liu, D. Schreurs, W. De Raedt, F. Vanaverbeke, R. Mertens, I. De Wolf, Thermal optimization of GaN-on-Si HEMTs with plastic package, Microelectronics Reliability, Volume 51, Issues 9–11, 2011, https://doi.org/10.1016/j.microrel.2011.06.033.

[36] Luoyun Yang, Baoxing Duan, Yintang Yang, Temperature optimization for AlGaN/GaN HEMT with the etched AlGaN layer based on 2-D thermal model, Solid-State Electronics,Volume 178, 2021, https://doi.org/10.1016/j.sse.2021.107982.

[37] Ahmed F. Al-Neama, NikilKapur, Jonathan Summers, Harvey M. Thompson, Thermal management of GaN HEMT devices using serpentine minichannel heat sinks, Applied Thermal Engineering, Volume 140, 2018, https://doi.org/10.1016/j.applthermaleng.2018.05.072.

[38] Mohanty, S.K., Chen, YY., Yeh, PH. *et al.* Thermal Management of GaN-on-Si High Electron Mobility Transistor by Copper Filled Micro-Trench Structure. *Sci Rep* **9,** 19691 (2019). https://doi.org/10.1038/s41598-019-56292-3.

[39] A. Haghshenas, M. Fathipour and A. Mojab, "Dependence of self-heating effect on passivation layer in AlGaN/GaN HEMT devices," *2011 International Semiconductor Device Research Symposium (ISDRS)*, 2011, pp. 1-2, doi: 10.1109/ISDRS.2011.6135303.

[40] Subhash Chander, Partap Singh, Samuder Gupta, D.S. Rawal, and Mridula Gupta, Self-heating Effects in GaN High Electron Mobility Transistor for Different Passivation Material, Defence Science Journal, Vol. 70, No. 5, September 2020, pp. 511-514, DOI : 10.14429/dsj.70.16360.

[41] Arivazhagan, L., Nirmal, D., Reddy, P.P.K. *et al.* A Numerical Investigation of Heat Suppression in HEMT for Power Electronics Application. *Silicon* (2020). https://doi.org/10.1007/s12633-020-00647-3.

[42] Silvaco, Atlas User's Manual Device Simulation Software; Silvaco, Inc.: Santa Clara, CA, USA, 2016;

[43] Keblinski, P.; Phillpot, S.R.; Choi, S.U.S.; and Eastman, J.A. (2002) Mechanisms of heat flow in suspension of nano-sized particles, International Journal of Heat and mass transfer, 45:855 - 863 , doi: 10.1016/S0017-9310(01)00175-2.

[44] Cahill, D.G.; Braun, P.V.; Chen, G.; Clarke, D.R.; Fan, S.; Goodson, K.E.; Keblinski, P.; King,W.P.; Mahan, G.D.; and Majumdar, A.; (2014) Nanoscale thermal transport. II. 2003–2012,applied Physics Reviews , 011305:1 – 45 , doi:10.1063/1.4832615

[45] Schubert, T.; Trindade, B.; Weißgärber, T.; and Kieback, B. (2008) Interfacial design of Cu-based composites prepared by powder metallurgy for heat sink applications, Materials Science and Engineering ,475:39–44 , doi:10.1016/j.msea.2006.12.146.

[46] Brendel, A.; Popescu, C.; Leyens, C.;Woltersdorf, J.; Pippel, E.; and Bolt, H. (2004) SiC-fibre reinforced copper as heat sink material for fusion applications,Journal of Nuclear Materials, 329–333 : 804–808, doi:10.1016/j.jnucmat.2004.04.304.

[47] Tekce, H.S.; Kumlutas, D.; and Tavman, I.H. (2007) Effect of Particle Shape on Thermal Conductivity of Copper Reinforced Polymer Composites, Journal of REINFORCED PLASTICS AND COMPOSITES, 26(1):113 – 121 ,doi:10.1177/0731684407072522

[48] A. M. Darwish, A. J. Bayba and H. A. Hung. (2004) Thermal Resistance Calculation of AlGaN–GaN Devices, IEEE TRANSACTIONS ON MICROWAVE THEORY AND TECHNIQUES,52(11): 2611 – 2620, doi:10.1109/TMTT.2004.837200

[49] Wang, X, and C.,Hu, G; (2005) Growth and characterization of 0.8-μm gate length AlGaN/GaN HEMTs on sapphire substrates, Science in China Ser. F Information Sciences ,48 (6): 808—814 doi:10.1360/122004-81.

[50] Y. Zhang, S. Feng, H. Zhu, C. Guo, B. Deng and G. Zhang. (2014) Effect of Self-Heating on the Drain Current Transient Response in AlGaN/GaN HEMTs , IEEE ELECTRON DEVICE LETTERS, 35(3):345 – 347 doi:10.1109/LED.2014.2300856.

[51] Yachao Zhang, Rui Guo, ShengruiXu , Jincheng Zhang, Shenglei Zhao, Haiyong Wang, Qiang Hu,ChunfuZhang , and Yue Hao. (2019) High-performance high electron mobility transistors with GaN/InGaN composite channel and superlattice back barrier, 115(072105):1-5 doi: 10.1063/1.5102080